Journal of Welding Technology
P-ISSN: 2716-1471 | E-ISSN: 2716-0475
http://e-jurnal.pnl.ac.id/Welding_Technology

Fillet weld strength analysis for cantilever loading: an investigation of single-sided fillet weld strength in bending applications

Tyler J. McPheron, Robert M. Stwalley III*
Department of Agricultural & Biological Engineering, Purdue University,
West Lafayette, Indiana, USA
*Corresponding author: rms3@purdue.edu

Article Processing Dates:
Received 2024-02-27
Reviewed 2024-04-12
Accepted 2024-06-26
Available online 2024-06-30

Keywords:
Bending
Cantilever loading
Crush test
Sample preparation
Welded joint

Abstract

Theoretical calculations for assessing the strength of a welded connection in design rely on two parameters: the tensile strength of the weld filler metal and the effective area. It is important to note that the type of load applied can significantly affect the theoretical strength of the weld. According to the AWS Structural Welding Code D1.1, when the load is applied parallel to the weld in a welded member, a reduction of 70% is recommended. This remaining factor of 0.30 has been determined through well-accepted tests to provide factors of safety between 2.2 for shearing forces parallel to the longitudinal axis of the weld and 4.6 for forces normal to the axis under service loading. When a load is applied perpendicular to the weld in a welded member, the entire value of the tensile strength of the weld filler metal is used to calculate the strength. However, there are no similar considerations for a load applied in a bending configuration. While it is not recommended for structural design, fillet welded members can experience loading that causes material deflection, resulting in a bending scenario. This is particularly relevant in repairs. The configuration of a cantilevered beam creates a different loading scenario with additional stresses on the weld, which differ from those of a perpendicular or parallel load. This research experiment was conducted to initially understand and analyze the strength of a GMAW weld under cantilevered bending and to derive a mathematical equation that provides a factor of safety in the range of 2.2-4.6, similar to the previous findings.

Nomenclature
A = effective weld area (in^2)
E_f = allowable stress factor / equation factor
F_t = weld strength (lb_f)
L_s = leg size (in)
L_w = weld length (in)
P_f = failure load from experiment (ultimate strength (lb_f))
W_t = theoretical throat thickness (in)
σ_t = ultimate tensile strength of weld filler (psi)

1. Introduction

The care and planning taken in the engineering design of a weldment for a mechanism may not always be present in the field repair of the same device, or the individual performing the repairs may be forced into a situation where the lesser of two evils necessitates doing something not optimal. The needed welding repair may not be in a position where both sides are accessible, or the repair personnel may not recognize the importance of a structural joint with good penetration on both sides of the repair. In either event, where only one edge of the two pieces is attached, single-sided welds can occasionally be produced, and they can ultimately carry cantilevered loads. Even though the scenario is less than desirable and not suggested, it would be appropriate if a generalized strength reduction for the situation was known. However, little seems to have been published on this state of affairs, other than to say it is not recommended.

Therefore, the research objective in this effort is to determine an initial quantifiable reduction in strength for a single-sided weld in a cantilever-loaded situation. The balance of this paper will consist of a section covering the background of the experiment and a literature review focusing on the subject, the methodology of the experimentation and the materials used to execute the work, the results of the testing and a discussion of the outcomes, and the conclusions about this effort and recommendations for further study.

Many established machine design texts include sections on welding processes [1-4]. They tend to concentrate on basic welded joints and ignore non-standard circumstances like those under consideration here. An understanding of various load configurations is provided in this section as background information to further aid in the analysis and testing of bending loads. This section of the paper will also examine prior investigative work done on cantilever loads and offer known information about limiting considerations of the study.

Simple loading conditions are divided into four respective categories: bending, axial, torsion, and transverse [4]. A shear loaded welded joint is defined by a force that is applied across the effective area of the weld in parallel with the length of the weld. A shear loaded weldment can be placed in either tension or compression. The free body diagram for this load scenario is shown in Fig. 1. There are additional considerations when evaluating the stresses and load capacity of welds loaded in the shear mode. This is due to the load being concentrated on the root penetration of the weld, without the structural support from the whole surface area of each weld leg attached to the base metal. This is the major difference between a parallel and a perpendicular loaded weldment.

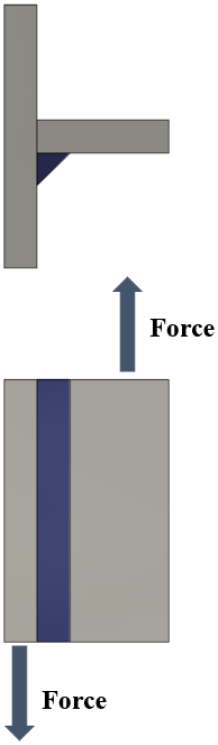

Fig. 1. Loads present in parallel or shear loaded weldments.

Transverse load is defined as a force applied in the transversal direction, or perpendicular to the effective weld area. This is also referred to as a tensile load. When loaded perpendicular to the weld axis, the weld is often significantly stronger than welds that endure shear load. When proper root penetration is achieved, a larger percentage of the weld material provides structural support to the joint in perpendicular loading. Fig. 2 provides an example of a transversely loaded weldment.

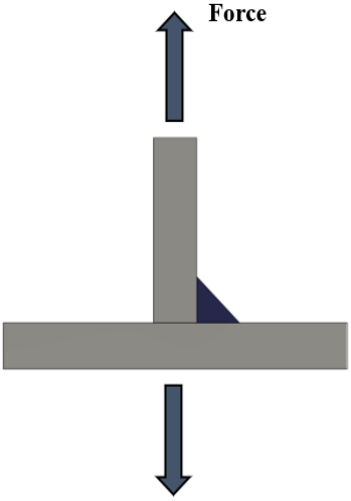

Fig. 2. Loads present in perpendicular or transverse loaded weldment.

A cantilevered beam is a structural member secured perpendicular to another structural member with one fixed end on the joint side and one free end, similar to the free body diagram in Fig. 3. A fixed end can be constrained perpendicular structural member by a variety of ways, such as bolted connections, pinned connections, or welded joints. This is a common configuration in structural design and is used in a variety of design applications for supporting a structural load. Cantilever beams can be made of any material. Steel beams, plates, and concrete are often used in structural applications. The term "beam" should be considered as an engineering term for the configuration of the structural member, not necessarily the shape and size of the material itself. A structural member is considered a beam if it is loaded perpendicular to its axis. Trusses are structural members that are loaded in the axial direction. Often, combinations of both trusses and beams make-up the core foundation of many small, engineered components, as well as large building structures. While not recommended for welded joint design, this cantilevered configuration can be present in many field repairs, where it is impossible to get to the opposite side of the weldment [5]. This effort was intended to provide quantitative information on how structural components with single sided welded joints would handle cantilevered loading. For this research experiment, a welded t-joint was constructed with steel plate serving as the cantilever beam. Stwalley and McPheron [6] previously reported on the design of this experiment. Computing deflections for the test pieces with an applied load was not part of the scope of current work.

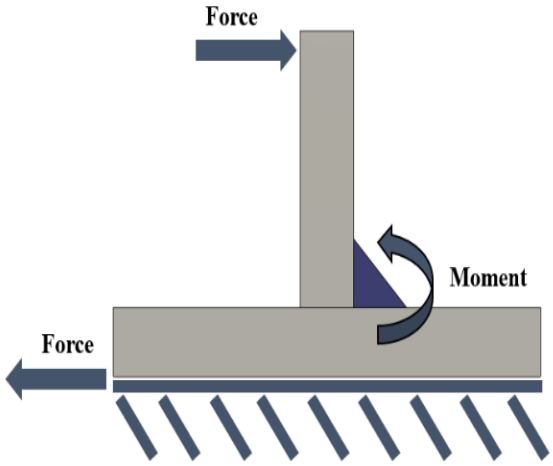

Fig. 3. Loads were present in cantilevered beams with one free end and one fixed end.

As expected, since this is a non-ideal joint, preliminary examination of the literature does not find many references to the specific cantilevered configuration under investigation in this study. Gomez et al. [7] provide a good primer on out-of-plane bending, and as shown in Fig. 4, categorize common loading scenarios for bending as 'in-plane' and 'out-of-plane'. There has been some experimentation with the out-of-plane scenarios, and design recommendations for this configuration exist [8]. However, as shown in Fig. 5, the current bending scenario under investigation could also be described as a combined load and torque placed onto the weld joint, and the weldment will have difficulties resisting deformation and failure under load. Clearly, the lack of exposition in the literature on this type of weld is due to the disadvantaged nature of the joint and its resulting valid criticisms [9-11].

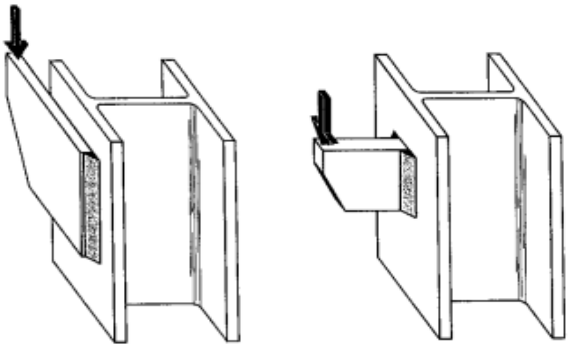

Fig. 4. Type of rotation induced by eccentric loads: in-plane on left and out-of-plane on right.

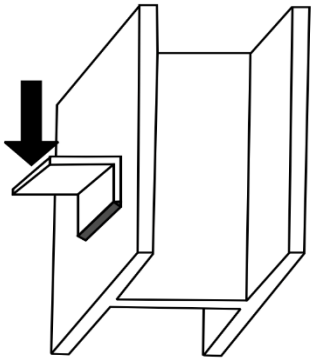

Fig. 5. Out-of-plane rotation induced by cantilevered scenario.

Where the cantilevered scenario is referenced in the literature, it is always with members having a deeper section than a simple solid bar or flange. Some work on square tubing and round tubing attached to channel pieces and placed in bending has been published [12-16], as well as a studies on deck panels welded to bridge ribs, which are subjected to cantilevered bending [17-18]. Studies have also been performed on strengthening this type of connection through the addition of small circles and diamond stiffeners [19]. From the section views in Fig.s 3 and 5, it can be seen that multiple problematic elements within standard welded construction will adversely affect any cantilevered welded joint. Welding has been demonstrated to affect the microstructure of the base materials in a joint [20], and imperfections in the welding process can certainly result in voids or inclusions creating a stress concentration within the weld, particularly with an inexperienced or poor welder. Stress concentrations in mechanical designs can be present for any number of unusual design or manufacturing features, including weldments [21-25]. Therefore, any type of stress concentration near the cantilevered joint could potentially have an amplified effect given the disadvantaged nature of this joint. This would adversely affect the long-term life of the weldment and the overall structure [26].

Although not directly influencing this study, it should be noted that welded joints are also susceptible to fatigue failure [27], and cantilevered joints by their nature are particularly vulnerable. The quality of a weld has been shown to dramatically affect its performance under repeated bending load conditions [28-29]. Multiple factors have been shown to affect weld quality [30-31]. Welding current and electrode angle have been shown to have a measurable effect on the uniformity of root depth [32-34], and inadequate penetration dramatically reduces the strength of a weld dramatically [35-36]. All factors reported in the literature that adversely affect weld strength are likely to have amplified effects in cantilever loading scenarios. A shallow root depth for the weld provides less weld area and leverage to resist bending. A poor weld creates imperfections that can enhance stress concentrations within or near the weld, augmenting the stresses inside the disadvantaged zone carrying the loads. This study was intended as an investigation to understand the level of that disability and to provide quantitative guidance regarding the level of strength reduction that can be expected under this cantilevered bending scenario.

This work was prompted by the lack of guidelines for field repair conditions which sometimes necessitate creating weldments that would not be utilized in new designs or in existing manufactured products. The experimentation was designed using historic investigations regarding weldment strength as reference [37-40]. Two sets of test pieces fabricated from two thicknesses of mild plate steel were used as experimental samples for weld bending testing.

The objectives of this study were determine if uniform, high quality test pieces could be fabricated for a single source sufficient for the welding bend test; determine if the thicker test pieces could bear a larger load than the thinner pieces; determine the load reduction factor for the test pieces in a cantilevered bending configuration; and determine if the load reduction factor was uniform between the two thicknesses of test pieces.

2. Methodology and Materials

Due to the significantly improved electrodes and steel material which became available during the late 1960s, scientific welding experimentation was conducted to update welding provisions and practices [37], from those used in the original structural steel design report from the 1930s [38]. The revised test, headed by Dr. A. Amirikian and conducted by a Task Committee of the AWS Structural Welding Committee, developed a suitable set of guidelines in 1968 [37]. It was concluded that a more conservative working stress of 0.30 times the tensile strength of the electrode material was justified for shear loading. This new recommendation revised the previous 0.60 value of the specified minimum yield stress of the steel for basic working stress used in structural steel design in 1931. The American Welding Society D1.1 Structural Welding Code cites Higgins & Preece [37] in C2.10 of D1.1 says that “a working stress equal to 0.30 times the tensile strength of the filler metal, as designated by the electrode classification, applied to the throat of a fillet weld has been shown by tests to provide a factor of safety ranging from 2.2 for shearing forces parallel to the longitudinal axis of the weld”. Table 1 lists the allowable stresses from AWS D1.1 Table 2.3 [39]. Since no such guidelines exist for the cantilever bending scenario, this experimentation seeks to provide some preliminary guidance. The balance of this section will describe the test piece fabrication process for the experimentation, the bending test procedure, the inspections, and the assumptions within the current investigation.

Table 1. Table 2.3 from AWS D1.1 (American Welding Society, 2000).

Fillet weld	Shear on effective area	0.30 x nominal tensile strength of filler metal[4]	Filler metal with a strength level equal to or less than matching filler metal may be used.
	Tension or compression parallel to axis of weld[3]	Same as base metal	

3.1 Experimental Procedures

The current experimental effort aimed to create a statistically relevant set of GMAW test pieces, in accordance with recommended testing processes, that could be used to begin an experimental exploration of fillet welds in bending. The fabrication process manufacturing the sample pieces for the crush testing was as controlled and uniform as possible, given the resources available for the work. It was established during the planning process that twenty samples with two weld sizes would be sufficient for an initial experiment. The American Welding Society Fillet Weld Break Test [40] was used to conduct a series of destructive tests in an effort to derive the allowable stress factor to be used for the weld strength design calculations to yield a consistent factor of safety for a fixed edge, cantilevered load scenario. Two plate thicknesses of 0.250 in (6.3 mm) and 0.375 in (9.5 mm) were evaluated by analyzing the relationship between ultimate strength and weld size in compliance with the AWS D1.1 welding code. Materials were acquired through the Purdue University Materials Acquisition Warehouse for:

Test Sample A: 0.250 in (6.3 mm) A36 Mild Steel Plate (Sample size = 20) and

Test Sample B: 0.375 in (9.5 mm) A36 Mild Steel Plate (Sample size = 20).

The statistical goal of the experiment was to record data from enough samples to calculate the standard deviation of the load at failure for each plate thickness. A consistent failure load amongst the 20 samples of each material thickness would provide the statistical basis for deriving an accurate allowable stress reduction factor for calculating the strength of welds subject to cantilevered bending. Material thicknesses of 0.250 in (6.3 mm) and 0.375 in (9.5 mm) were specifically chosen, due to the increase in weld leg size defined in AWS D1.1, as shown in Table 2 for the larger thickness plate. The percent increase in weld size will be compared with the percent increase in strength for the larger weld size of the two samples. One of the finished 0.250 in (6.3 mm) 'A' test samples is shown in Fig. 6.

Table 2. D1.1 Weld Leg Size Specifications (American Welding Society, 2020).

Test Material Thickness (in)	*Leg Size*	*Size (in)*
0.250	Minimum	0.125
0.375	Minimum	0.1875

Fig. 6. A12 test specimen for fillet weld bending experiment.

The test sample manufacturing protocol and testing process for the bending experiment was defined with the following fabrication steps:

1. Weld Preparation & Welding

1.1. Grind-off all mill-scale. Mark all component pieces for assembly and clamp them to the welding surface in the same manner using C-clamps and lockjaw pliers. Electrically ground the pieces in the same position for the welding process on each test specimen.

1.2. Set the Miller Multimatic® 255 welder (Appleton, WI) [41] to DC electrode positive and provide an Ar75/$CO_2$25 shield gas connection to the machine. Use 19.8 *volts* and 405 *in/min* (1030 *cm/min*) wire feed settings for the 0.250 *in* (6.3 *mm*) test pieces and 21.9 *volts* and 410 *in/min* (1040 *cm/min*) wire feed settings for the 0.375 *in* (9.5 *mm*) specimens.

1.3. Use the GMAW process to weld two A36 mild steel plates together in a tee-joint configuration welded on one side of the joint, as in Fig. 7.

1.4. Visually inspect the weld for excess porosity and undercut. Void the test specimen, if such inclusions are visible.

1.5. Cut a 1-inch cross-section of the test specimen on both ends of the test specimen with a power hack saw.

1.6. Measure the size of the fillet weld on the remaining 6 *in* (15 *cm*) test specimen with a fillet weld gauge, as in Fig. 8, or with dial calipers, shown in Fig. 9, for a more precise measurement. The fillet weld size must be uniform for entire weld length. Photograph and record measurement according to test specimen number.

Fig. 7. Plate configuration for welding pieces into fillet weld bending experiment test sections.

Fig. 8. Measuring fillet weld with manual fillet weld gauge.

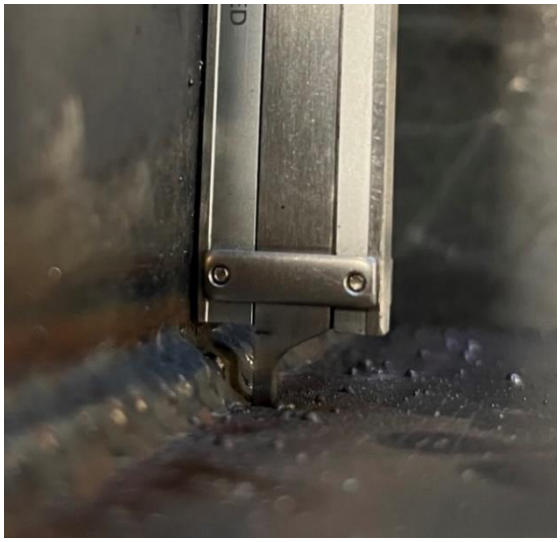

Fig. 9. Measuring fillet weld with dial calipers for more precision.

2. Macro-etch Test

   2.1. Grind and polish the welded joint area on one of the 1 *in* (2.5 *cm*) cross-sections.

   2.2. Apply phosphoric acid to the welded joint, while joint is still warm from polishing.

   2.3. Allow 2 *min* to let the phosphoric acid etch the weldment.

   2.4. Visually inspect the joint for adequate root fusion and equal fusion into the base metal. Photograph and record the root fusion.

3. Repeat steps 1.1 - 2.4 for 40 test specimens.

   3.1. Number each test specimen for tracking purposes. Assemble the samples for transport to the test site at the Purdue Pankow Laboratory, as shown in Fig. 10.

Fig. 10. Weld test specimens for bending experiment with Sample A on left and Sample B on right.

4. Data Collection

   4.1. Install the test specimens, oriented like Fig. 11, into an MTS Systems (Eden Prairie, MN) Insight electromechanical press, using rapid travel to bring the head into contact with the test piece. Following contact, zero the data logging equipment to eliminate any offsets. Start the real-time data logger to record and plot load and displacement.

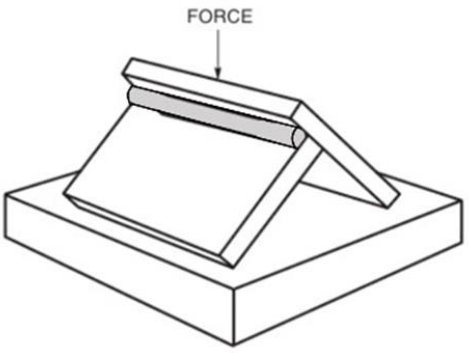

Fig. 11. Fillet weld break test configuration for bending experiment (American Welding Society, 2020).

   4.2. Apply continuous loading to the test specimen within the press, until the load / displacement curve is completed.

   4.3. Remove test specimen and inspect the edge of the break for root fusion in compliance with the AWS D1.1 visual inspection criterion for a fillet weld break test.

5. Repeat steps 4.1 – 4.3 for each sample of the various 0.250 *in* (6.3 *mm*) test specimens within each category of size. Then repeat the process for the other set of associated 0.375 *in* (9.5 *mm*) test samples.

All the test piece fabrication was performed at the Purdue University Agricultural & Biological Engineering ADM Student Achievement Center during the fall of 2022 by Tyler J. McPheron. To achieve minimal deviation between samples, each test specimen was conFig.d and hand-welded with consistent positions and machine settings. Preliminary test tee-joints were fabricated to adjust the welding machine for optimal performance. A macro-etch test was conducted on the test tee-joints to evaluate the root fusion for different machine settings. The final welding machine specifications are shown in Table 3, with some uncertainty and adjustment tolerance noted, due to building current draw and minor machine error.

Table 3. Welding equipment specifications for manufacturing welding bend test sections.

Welder	**Miller Millermatic® 252 MIG Welder**	**230V**
Voltage (*V*)	19.8 ± 0.5 (For ¼ *in* material)	21.9 ± 0.5 (For 3/8 *in* material)
Wire Feed Speed (in/min)	405 ± 10 (For ¼ *in* material)	410 ± 10 (For 3/8 *in* material)
Shielding Gas	25% Argon, 75% CO_2	-
Filler Metal	E70S Filler Wire (70,000 *psi*)	-
Filler Metal Diameter	0.035 *in*	

Each test specimen was placed in the same position on the welding table with the ground clamp placed in the same location for all samples. Each test specimen was welded in the 2F horizontal position, with a slight support underneath the specimen for a partial 1F flat welding position. The specimen was conFig.d this way for welder comfort. Fig. 12 shows a test specimen set-up for manufacturing.

Fig. 12. Welded test specimen for bending experiment ready for initial inspection.

3.2 Specimen Inspection Details

Table 4 details the bending test equipment used in this experiment. An MTS Systems (Eden Prairie, MN) Insight electromechanical press, shown in Fig. 13, was the primary piece of equipment used to carry-out the weld break test experiment. The MTS press had a 300 *kN* capacity rating (67,400 lb_f). A preliminary finite element analysis (FEA) study was conducted to estimate the amount of force required to break each test specimen or achieve the ultimate strength on the stress/strain curve. The FEA results showed that the joint would fail at approximately 5,000 lb_f (22.2 *kN*). This preliminary calculation ensured that the MTS press would be sufficient for testing the fillet weld specimens. The MTS press was paired with Labworks (Lehi, UT) software capable of actively plotting the load / displacement curve for each sample. The output values provided a large amount of as-measured data values for each test specimen, thereby meeting the experimental objectives for statistically valid testing.

Table 4. Equipment for data collection and testing welded samples in fillet weld bending experiment.

Description	**Mfg./Model**	**Specification**
Electromechanical Press	MTS Insight	300 kN Standard Length
Load Cell	MTS – 569331-01	300 kN Capacity
Software	Labworks	-

Fig. 13. MTS Systems (Eden Prairie, MN) Insight electromechanical press used in fillet weld bending experiment.

The American Welding Society has defined criteria for the inspections necessary before and after a fillet weld break test has been conducted. Before destructive testing of the test specimen, visual inspections should be completed by a certified welding inspector (CWI). The weld should be reasonably uniform throughout the length of the weld and

feature no exterior cracks, excess undercut, or porosity [39]. Assuming the specimen clears the visual inspections, the test is considered a pass, even if the specimen bends flat upon itself. Many engineers believe that a failed test occurs if the weld fractures. However, if the weld fractures on the centerline of the weld throat, shows complete fusion to the joining base metals, has no inclusion or porosity larger than 0.094 *in* (2.5 *mm*) in its greatest dimension, and the sum of the greatest dimensions of all inclusions and porosity do not exceed 0.375 *in* (9.5 *mm*) in the 6 *in* (15 *cm*) long specimen, then the test specimen is considered to have passed [39]. It should be known that it is common for the fillet weld to fracture during this test, especially if the base material is 0.500 *in* (12.7 *mm*) or thicker.

A macro-etch test was conducted by applying an acidic metal etching chemical to a cross-section of the fillet weld. A variety of chemicals can be used to achieve the etched conditions. In this experiment, a 37% phosphoric acid solution was used to macro-etch test each test specimen. Many welds can look uniform and structurally sound on the exterior, but they may have hidden imperfections underneath. The macro-etch test is used to ensure that the proper root fusion in the joining material is achieved. AWS specifies that the weld shall show fusion to the root of the joint, but not necessarily in excess amounts [39]. Excessive root fusion can weaken the joint significantly, and it can cause unacceptable amounts of undercut. This usually indicates too much current on the machine setting or a slow electrode travel speed. The true leg size of the weldment should also be measured at the time of the macro-etch test.

3.3 Experimental Assumptions

There are certain assumptions necessary to complete the logic chain for the bend testing analysis. The purpose for using the AWS fillet weld break test was to validate the data collected by implementing standard welding procedures. The standardized testing procedure [39] was followed to evaluate the 20 samples of 0.250 *in* (6.3 *mm*) tee-joint test specimens and 20 samples of 0.375 *in* (9.5 *mm*) tee-joint test specimens and establish a connection to the historically performed experimental weld testing procedures. The overall process validated the data collected and provided the basis for a scientifically binding experiment and conclusions. Additional considerations undertaken were to follow the accepted procedures, measure the necessary parameters outlined by AWS testing criteria, and be willing to exclude any non-compliant test specimens from the results to ensure the validity of the data collected in the experiment. It should be noted during this experiment that a non-certified, but experienced, welder fabricated the test specimens. In comparison, the 1968 Task Committee of the AWS Structural Welding Committee sent test specimens to a variety of different certified welders in different regions in the United States to ensure uniformity. The ideal scenario would be to program and use a robotic welder to fabricate all the test specimens examined in the experiment, but this was a preliminary study, and the resources for this experimentation were limited.

The purpose in using the AWS fillet weld break test was to authenticate the results by implementing standard welding procedures to collect the data, while following a standardized bend testing procedure for the samples of 0.250 *in* (6.3 *mm*) tee-joint test specimens and samples of 0.375 *in* (9.3 *mm*) tee-joint test specimens. The AWS D1.1 procedure for the fillet weld break test calls for the test specimen to be quenched in water directly after the weld is completed. The test specimens used in this experiment were not quenched after welding to ensure that the full tensile strength of the weld material was considered for analysis. AWS requires weld quenching for certification tests which allow the weld to break easier. Not quenching the test specimens can alter the way the weld breaks, since the weld filler metal has a higher tensile strength than the base metal. Certified welding inspectors do not measure failure load for the fillet weld break test, because most of the focus is on visual inspection and observation. These tests are completed to evaluate the welder's ability to join two materials, while maintaining proper weld size and adequate root fusion within the joint. These parameters can be measured more accurately, if the weld breaks at the center of the root. Under those circumstances, more attention is directed toward the inspection, if the break favors one side or the other. In this experimental investigation, loading at failure was of direct interest.

4. Results and Discussion

The measured values for the bend break weld tests of the fabricated specimens included load, time, and crush head extension of the press. Each test specimen was fixtured in the MTS machine in the same orientation, matching the AWS fillet weld break test loading criteria. The data recording equipment was then zeroed using the software program, before beginning the test. The test began by applying a continuous load to the test piece. These tests produced the load / displacement curves for each specimen, containing the maximum amount of load each sample absorbed before fracture [4]. Fig. 14 presents the results for test specimen A7, which were typical. The highest load was typically reached within the first few seconds of initializing the test. The crushing was stopped, once the load declined to 1,000 lb_f (4.4 *kN*). These steps were repeated for all 0.250 *in* (6.3 *mm*) thick and all 0.375 *in* (9.3 *mm*) thick test specimens. Fig. 15 shows a crush test in progress. The remainder of this section will discuss the bend break testing, the root fusion inspections, the statistical analysis of the bend test data, a comparison of the loading results between the two sample sizes, and an initial estimate of the proposed strength reduction design criteria, based upon the current experimentation.

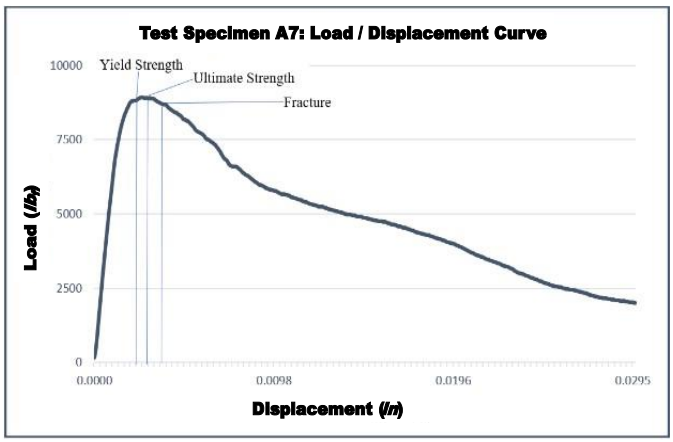

Fig. 14 - Stress/strain curve for A7 test specimen in fillet weld bending experiment.

Fig. 15. Test specimen in MTS Systems (Eden Prairie, MN) Insight electromechanical press during fillet weld bending experiment.

4.1 Bend Break Testing

The loading results at failure were recorded for each test specimen. Consistent results were achieved for the 0.250 *in* (6.3 *mm*) thick A test specimens, with a mean failure load value of 6,640 lb_f (29,500 *N*) and a standard deviation of 909 lb_f (4,040 *N*), resulting in a coefficient of variation of 0.137. This was a good result, considering the amount of potential error that can occur by manually welding each test specimen. It was also interesting to note that the A7 sample featured a slightly smaller weld size than the rest of the samples, yet it failed above the sample average failure load at 7,010 lb_f (31,200 *N*). This was an initial indication that there can be several variables that affect the strength of a weld, rather than just the effects of increasing or decreasing the weld size. It could be that there was a greater root penetration in the weldment, producing a small leg size, since more weld material would be concentrated within the joint in that case.

Table 5 shows the aggregate summary results for 0.250 *in* (6.3 *mm*) thick A test specimens and the 0.375 *in* (9.3 *mm*) B test specimens. Results for the B test specimens were less uniform than the results for the thinner A test specimens. However, for the size of the sample, these results will suffice. The potential error from manually welding and preparing each test sample created a large variability in results. The mean failure load for sample B was 12,400 lb_f (55,160 *N*), with a standard deviation of 1,600 lb_f (7,120 *N*), resulting in a coefficient of variation of 0.129. Even though the average size of the weld for B sample was only 12% higher than the average weld size for A samples, a 60% increase in ultimate load capacity was observed for the larger pieces. It is important to clarify that the results presented represent the raw, unfiltered data for the experiment. This data had not yet been cleaned and evaluated for sample failures and outliers that could potentially skew results, and therefore, was not used for the study's statistical analysis of the experiments.

4.2 Break Test Root Fusion Inspections

The MTS electromechanical press did not typically break the test specimens apart during testing. The load was lifted from each test specimen, once it decreased to 1,000 lb_f (4.4 *kN*). If the test specimen were to break before the end of the load curve, this would indicate a very weak weld with little penetration. Each tee joint was manually separated for further inspection. The main objective for the fillet weld break test was to examine root penetration at the joint and the distribution of weld metal within the base metals. This was done by separating the tee joint and inspecting the break. A clean break directly down the center axis of the weld indicated that there was an equal distribution of weld metal on both joining materials. This also implied that root penetration was symmetric and did not favor one side of the joint or the other. Favoring either leg was an indication that electrode angle was either too steep or too shallow in relation to the joint at that point. Table 6 presents the overall weld failure points for specimen testing.

Table 6. AWS fillet weld break test acceptance criteria (American Welding Society, 2000).

The broken specimen shall pass IF:	
(1)	The specimen bends flat upon itself.
(2)	The fillet weld, if fractured, has a fracture surface showing complete fusion to the root of the joint.
(3)	No inclusions or porosity larger than 3/32 in (2.5 mm) in its greatest dimension
(4)	The sum of the greatest dimensions of all inclusions and porosity shall not exceed 3/8 in (10 mm) in the 6 in (15 cm) long specimen.

Two of the tee joints failed inspection, due to excessive undercut. Undercut is an area of concentrated penetration into the base metal, usually at the toe of the weld, creating a visible crevice, further reducing the strength in this area significantly. The two rejected pieces with undercut were likely caused by welding too quickly. All pieces were fabricated by a single welder working under a deadline. The psychology of manufacturing so many test pieces for a time-constrained graduate-level academic experiment certainly could have created these flaws. Fig. 16 shows one of these deficient weldments. Eleven other tee-joints failed inspection, due to lack of root penetration. It is important to emphasize that there cannot be any amount of area along the joint that does not fuse into both base metals. Most of the failed tee-joints had only 0.125 *in* (3.2 *mm*) to 0.250 *in* (6.3 *mm*) length of effective weld area without proper root fusion, but this is still unacceptable for the bend testing and validation purposes. The cause of the penetration issues was also likely human error, with the torch tip being incorrectly aligned with the test pieces and concentrating filler metal on the bottom plate, rather than creating an even distribution having good penetration. Fig.s 17 and 18 present examples of failed weldments with insufficient root penetration.

Fig. 16. Undercut on Failed B11 Test Specimen in fillet weld bending experiment.

Table 5. Measured data summary statistics for the two thickness treatments with the fillet weld bending experiment.

Sample	*Material Thickness (in)*	*μ Leg Size (in)*	*μ Throat Size (in)*	*μ Failure Load (lb_f)*	*Failure Load Std. Dev. (lb_f)*
A	0.25	0.247	0.175	6,641	909
B	0.375	0.278	0.196	12,371	1,603

Fig. 17. Failed A1 Test Specimen through lack of fusion into bottom plate during fillet weld bending experiment.

Fig. 18. Failed A1 Test Specimen through lack of fusion into bottom plate during fillet weld bending experiment.

4.3 Statistical Analysis

To analyze the overall results of the experiment, four statistical tests were performed. Each research question was articulated to analyze one of the key objectives of the experiment. These tests, along with their hypothesis are shown in Table 7. There was enough data to do multiple analysis relating to the load and displacement curves produced for each sample. However, the primary focus for this experiment was on the ultimate strength of the weld in failure loading, the effective area of the weld, and the relationship between calculated theoretical strength and measured ultimate strength. All statistical tests were performed using R programming language for statistical computing.

Table 7. Statistical analysis research statement summary for fillet weld bending experiment.

Statistical Overview
1. Failure Load vs. Effective Weld Area
Is there a difference between failure load (lb_f) of 0.25" tee joints (sample A) and 0.375" tee joints (sample B) due to the difference in required weld sizes for the two base material thicknesses? $\boldsymbol{H_0}$: Sample A failure load = Sample B failure load $\boldsymbol{H_a}$: Sample A failure load < Sample B failure load Test: Two-Sample T-Test
Are there any significant outliers for failure load (lb_f) due to possible impurities in the weld for each sample of tee joints? $\boldsymbol{H_0}$: Significant outliers for failure load for both samples = 0 Test: Identify Outliers
2. Allowable Stress & Design Factor
Is there a difference between calculated equation factors between sample A and sample B? $\boldsymbol{H_0}$: μ equation factor for sample A = μ equation factor for sample B $\boldsymbol{H_a}$: μ equation factor for sample A ≠ μ equation factor for sample B Test: Two sample T-Test
Can an accurate conclusion be found as an acceptable equation factor for use in the design of components featuring welded joints loaded in a cantilevered bending configuration? $\boldsymbol{H_0}$: μ difference of equation factor between sample A and sample B = 0 Test: Comparison of means

4.3.1 Normality of Data

To prove the normality of the data samples, a Shapiro-Wilks test was performed for the raw data samples and the cleaned data samples with the failed test specimens removed. A p-value greater than the significance level of α=0.05 was observed for all sample scenarios under Shapiro-Wilk testing. The data with the removed test specimens remained normally distributed, and the exclusion of the failed samples did not change the distribution of the data sets. Results of the normality test are presented in Table 8.

Table 8. Shapiro-Wilk data normality test results for fillet weld bending experiment data.

Sample A	
Raw Data	P-Value = 0.727
Cleaned Data	P-Value = 0.121
Sample B	
Raw Data	P-Value = 0.434
Cleaned Data	P-Value = 0.086

4.3.2 Raw Data vs. Cleaned Data

Failed post-fabrication inspections in compliance with AWS D1.1 inspection criteria eliminated 13 of 40 test specimens, due to either a lack of root fusion observed after the break or a lack of root fusion observed when performing the macro-etch test before the break test. Five of the failed pieces were in sample A and eight of the failed pieces were in sample B. This left 15 specimens for sample A and 12 specimens for sample B. However, there were some interesting findings that come from comparing the raw data with the clean data for both samples.

It might have been reasonably expected to see a lower failure load from the test samples that were not compliant with the standards, but that was not necessarily the case during this experimentation. Many of the failed test samples failed within a reasonable amount of variance from the cleaned sample mean. Another anomaly in the results included test specimens that inspected quite well, but failed at a lower load than other test specimens that failed inspection. For example, sample B12 failed at 9,470 lb_f (42,100 *N*), but it showed adequate root fusion, a uniform weld, and a break which ran down the center axis of the weld. The lowest measured failure load from the rejected test specimens in sample B was measured at 10,230 lb_f (45,500 *N*). Table 9 contains statistical summaries for the failed test specimens, comparing them against the passing test specimens.

Table 9. Summary statistics for samples A & B in the fillet weld bending experiment.

Sample A			***Sample B***		
Failure Load	***Inspection: P/F***	***Load (lb_f)***	***Failure Load***	***Inspection: P/F***	***Load (lb_f)***
μ	Pass	6,870	μ	Pass	12,546
μ	Fail	5,956	μ	Fail	12,110
Max	Pass	8,411	Max	Pass	15,360
Max	Fail	7,449	Max	Fail	14,592
Min	Pass	5,930	Min	Pass	9,474
Min	Fail	4,947	Min	Fail	10,231

The passing test specimens characterized the population well, even following the sample size reduction from removing the failed test specimens. The summary statistics were re-analyzed to validate the reliability of the smaller sample sizes, after removing the failed test specimens. The normality check using the Shapiro-Wilks test confirmed that the cleaned data was adequately normal to perform the remaining statistical comparisons tests for the experiment.

4.3.3 Outliers from Defects & Impurities

A comparison of the results for the bending experiment of the failed verses passed sample pieces is presented in Table 10. There were no significant outliers identified by performing an outlier's test on the raw data for sample A and sample B. This analysis considered all 40 tee joint test specimens. A box plot, shown in Fig. 19, was used to identify any outliers that might have been present in the data. The lack of outlier detection in the raw data inferred that none of the 13 test samples that failed the AWS root fusion inspection were actually statistical outliers. Furthermore, the mean ultimate strength of the samples that failed the fillet weld break test inspections did not deviate significantly from the mean ultimate strength of the test samples that passed the fillet weld break test inspections. Therefore, it can be concluded that minor amounts of non-existent root fusion, undercut, and impurities do not reveal themselves as significant outliers or have a direct correlation to ultimate strength. However, it may be assumed that multiple imperfections or the lack of root fusion, such as for more than 25% of the effective weld area, would likely cause a notable reduction in ultimate strength.

Table 10 - Comparison of pieces tested with passing means vs. pieces tested with failing means in fillet weld bending experiment.

Sample A	
Mean Ultimate Strength	6,870 lb_f
Mean Ultimate Strength of Failed Samples	5,956 lb_f
Sample B	
Mean Ultimate Strength	12,546 lb_f
Mean Ultimate Strength of Failed Samples	12,110 lb_f

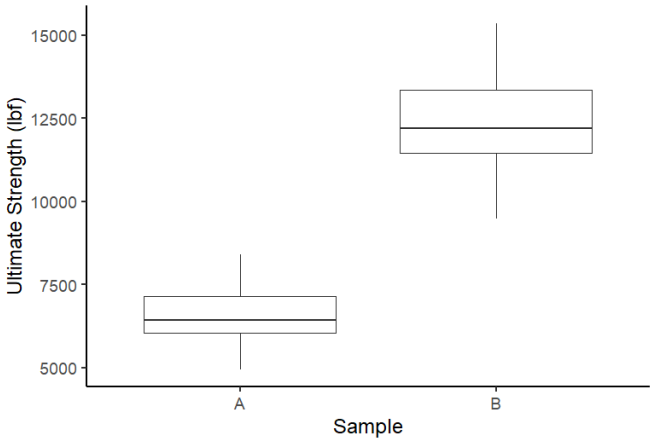

Fig. 19. Uncleaned data outlier detection test for fillet weld bending experiment.

Despite the lack of statistical outliers in the weld bend test specimens, there were a few interesting occurrences to note. Test sample B12 showed an ultimate strength of 9,470 lb_f (42,100 *N*). This was well below the mean ultimate strength of 12,550 lb_f (55,800 *N*) for the samples that passed inspection, yet the B12 sample inspected well, with a uniform break through the center axis of the weld and adequate root fusion at the joint. The premature failure compared to the rest of the samples could have been caused by a subtle variation when fixturing in the MTS machine or by quality issues within the steel material, particularly that the grain direction was not considered when making the samples. Another potential reason for premature failure might include an improper fit-up during fabrication prior to welding. There were no visible imperfections or quality issues with this sample, but its substandard performance was noteworthy. Fig. 20 and 21 show this unique specimen.

Fig. 20. B12 test specimen from the fillet weld bending experiment.

Fig. 21. Fracture down the center of the weld axis of the B12 test specimen from the fillet weld bending experiment.

4.4 Failure Load vs. Effective Weld Area

For the 0.250 *in* (6.3 *mm*) and 0.375 *in* (9.5 *mm*) plate thicknesses evaluated in the experiment, different weld size standards were specified and created during the fabrication of the samples. An exact measurement of the produced weld is vital to estimating its strength. Fig. 22 displays some tools for weldment measurement. Fig. 23 illustrates the relative geometry of the weldment under study, and equations [1] and [2] define the basic parameters of throat thickness and effective weld area. Table 11 shows that the fillet weld leg size can be a minimum of 0.125 *in* (3.2 *mm*) for a fillet weld on 0.250 *in* (6.3 *mm*) material [39]. The fillet weld leg size can be minimum of 0.188 *in* (4.8 *mm*) for a fillet weld on 0.375 *in* (9.5 *mm*) material [39]. Previous editions of AWS D1.1 Structural Welding Code specified a maximum leg size for different material thicknesses, but this constraint has been removed in recent revisions of the code. Unfortunately, this revised guideline does not then constrain over-welding.

Over-welding can be very costly for manufacturers of welded parts. Over-welding does not increase the strength of the joint, and in some cases, it may noticeably weaken the joint. Welders and engineers use a common rule of thumb for a fillet weld leg size that is 75% of the base metal thickness. This maintains adequate strength, while minimizing over-welding [42]. In this experiment, all fillet weld leg sizes were measured with dial calipers and fillet weld gauges to accurately quantify the leg size for each test specimen. Fillet weld gauges are good tools for taking quick measurements, but they have limited accuracy. A measurement of 0.001 *in* (0.0025 *mm*) can be obtained by using dial calipers. Obtaining the leg length and the overall length of the weld for each test specimen provided the necessary measurements to calculate the effective weld area for each test specimen under Equations 1 and 2.

Fig. 22. Fillet Weld Measurement Tools.

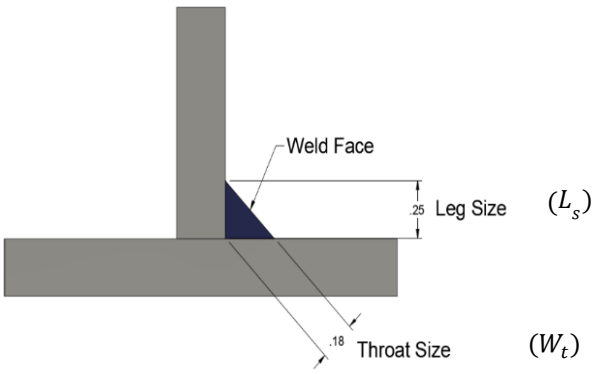

Fig. 23. Cross-Section of Fillet Welded Tee Joint.

$$W_t = (\cos(45°)) * L_s \quad [1]$$

$$A = W_t * L_w \quad [2]$$

Where W_t is theoretical throat thickness (in), L_s is leg size (in), A is effective weld area (in^2), L_w is weld length (in).

Table 11 - Welding leg sizes for samples A & B for the fillet weld bending experiment.

Sample A	
Min Weld Leg Size	0.1875 in
μ Weld Leg Size	0.246 in
μ Effective Weld Area	1.044 in^2
Sample B	
Min Weld Leg Size	0.250 in
μ Weld Leg Size	0.278 in
μ Effective Weld Area	1.187 in^2

4.4.1 Failure Load vs. Effective Weld Area Analysis

The mean failure load for the thicker 0.375 in (9.5 mm) test specimens in sample B was approximately twice the mean failure load observed for the 0.250 in (6.3 mm) test specimens in sample A. Due to these significantly different results, the hypothesis that failure load was equal, despite the larger weld size and thicker base materials, would be rejected. Table 12 provides the details of these statistical results. It is difficult to tell from these results if the plate thickness or the effective weld area influenced the strength of the weld more than the other. Fig. 21 showed the simplified cross-section of a fillet welded tee joint. However, this is not the realistic shape of an appropriate weld. If the weld was completed properly, the theoretical size of the weld throat should be a close approximation to the actual weld size, but it is typically less than the actual weld size. Additionally, the increased weld size in sample B for the larger plate thickness compared to sample A was likely a contributing factor to the sample B average failure load being twice the ultimate average load capacity of sample A. Larger base metal thicknesses provided greater structural area and support for the joint, when bend tested in the fixturing configuration used for this experiment.

Table 12. Statistical summary of results for failure load vs. effective weld area for fillet weld bending experiment.

Two-Sample T-Test

Sample	*Mean (lb_f)*	*Std Dev (lb_f)*	*P-Value*	*t-Value*	*DF*	*Min (lb_f)*	*Max (lb_f)*
A	6,870	774	p<0.001	-11.81	25	5,930	8,411
B	12,546	1,654	p<0.001	-11.81	25	9,474	15,360

The difference between the theoretical throat size in Fig. 21 and the larger actual throat size shown in Fig. 24 is notable. The root depth and penetration into the base materials is greater in the thicker specimens. The additional material thickness in sample B is a secondary contributor to the increase in strength measured in the experiment. The mean difference in effective weld area between sample A and sample B is 0.143 in2 (0.923 cm2) with a weld leg size difference of 0.032 in (0.810 cm). With just over 0.0312 in (0.79 cm) difference between the two samples, this variance might seem negligible. However, the small difference showed profound results, when comparing the calculated theoretical load capacity for both weld sizes.

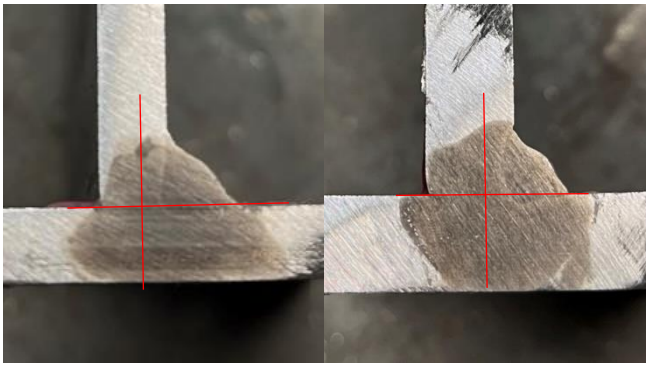

Fig. 24. Sample A macroetch test vs. Sample B macroetch test for fillet weld bending experiment.

4.4.2 Theoretical Strength for Transverse Loading

Equation [3] provides the means to determine weld strength. By using the previous equations, with a 0.0312 in (0.79 cm) larger leg size, a 13% increase in theoretical strength was observed. The additional 37% increase in strength seen in the experiment can be credited to the bigger 0.375 in (9.5 mm) plate thickness. Larger weld sizes have an indirect effect on the strength of a welded connection when subject to cantilevered bending. However, because of the loosely defined standards provided by AWS for weld sizes dependent upon plate thickness, there are still several unknowns as to the effect of plate thickness on strength of the welded connection. A better experiment for this test would be to compare two samples with plate thicknesses inside of the same base metal thickness interval defined by AWS for one singular weld size. For example, according to AWS D1.1, the minimum leg size required for welding both 0.125 in (3.2 mm) and 0.188 in (4.8 mm) thick base metal is 0.125 in (3.2 mm).

$$F_t=\sigma_t*A \qquad [3]$$

Where F_t is weld strength (〖lb〗_f), σ_t is ultimate tensile strength of weld filler (psi), A is effective area of the weldment (in^2).

Testing two samples with these specifications would likely lead to a better indication of the influence that plate thickness has on joint strength. This experiment used 0.250 in (6.3 mm) and 0.375 in (9.5 mm) thick base metals, which require two different minimum weld leg sizes. Therefore, there are two confounding factors potentially influencing the strength of the weld [6]. Calculated weld strengths for the two plate thicknesses are dependent upon the measured weld area and projected strength of the resolidified melt volume. Uncertainty in the outcome could come from errors in measurement and variance in projected strength. The latter is likely to be a larger factor, since the strength of the resolidified pool is dependent upon multiple factors which

could result from the heating and cooling processes. Using the 6 in (15.2 cm) sample length and average measured leg size of the specimens from Table 11, the estimated effective area for Samples A and B is 1.044 in2 (6.735 cm2) and 1.187 in2 (7.658 cm2), respectively. Specimen strength is calculated as:

Sample A: $73{,}080\ lb_f = 70{,}000\ psi * 1.044\ in^2 = 325\ kN$
Sample B: $83{,}090\ lb_f = 70{,}000\ psi * 1.187\ in^2 = 370\ kN$

4.5 Allowable Stresses & Design Factor

The allowable stress for fillet welds loaded perpendicular to the weld axis is the same as the ultimate tensile strength of the filler metal. The weld filler metal is the material that gets melted into two base materials to join them together. Filler metals are used in all welding processes and must have better or equal mechanical and chemical properties than the base material being welded [43]. Most filler metals used for welding mild low-carbon steel feature an ultimate tensile strength between 60 ksi (414 MPa) and 70 ksi (483 MPa). However, as previously mentioned, AWS D1.1 Clause 4 requires a 70% reduction in the allowable stress for evaluating fillet welds loaded in the shear direction [39]. This allowable stress reduction metric yields safety factors of 2.2 for parallel forces to the weld axis to 4.6 for forces normal to the weld axis [44]. Fig.s 1 and 2 provided a comparison between transverse and shear loading configurations. To reduce the allowable stress by 70%, the ultimate tensile stress of the filler metal used to produce the weld being evaluated is multiplied by 0.30, as shown in equation [4]. This value was derived from the experiments outlined in Higgins & Preece [37].

$$F_t = 〖(\sigma〗_t * 0.30) * A \quad [4]$$

Where F_t is weld strength (〖lb〗_f), σ_t is ultimate tensile strength of weld filler (psi), A is effective area of the weldment (in^2).

4.5.1 Allowable Stress in Tee-Joint Welding Tests

The factor for the allowable stress used for estimating the strength of a fillet weld in a bending configuration can be derived by rearranging equation [4] into equation [5]. This equation uses the failure load recorded in the experiment for each test specimen, along with its corresponding measured effective weld area. Table 13 provides the results of this experiment in the form of a similar strength reduction stress factor. Using this methodology, the 0.250 in (6.3 mm) specimens produced a reduction factor of 0.10, and the 0.375 in (9.5 mm) samples yielded a 0.15 factor. As expected, both values are significantly lower than the full-strength transverse loading factor. The cantilevered loading produced a stress reduction factor 50% smaller than that for shear loading.

$$E_f = P_{ultimate} / (\sigma_t * A) \quad [5]$$

Where E_f is allowable stress reduction factor, P_ultimate is failure load from experiment [ultimate strength] (lbf), σ_t is ultimate tensile strength of weld filler (psi), A is effective area of the weldment (in^2).

Table 13. Calculations with averaged test measurements for fillet weld bending experiment.

Sample	Failure Load (lb_f)	Stress (psi)	Tensile Strength (psi)	Effective Weld Area (in^2)	Stress Factor -
A	6,870	8,640	70,000	1.044	0.10
B	12,546	15,97	70,000	1.187	0.15

4.5.2 Allowable Stress Experiment Statistics

Results for a consistent allowable stress reduction factor between the two samples were not equal. For this experiment, it can be concluded that hypothesis of equal allowable stress factors calculated from the data should be rejected. A reduction of 90% and 85% for the allowable stress at the welded connection is shown by the data. This is significantly different than the 70% reduction in shear, with forces acting upon the weld axis in parallel. It is clear that the bending scenario illustrated in this experiment does not compare well to strength values from welds loaded in shear and transverse conditions. To use this factor in a structural design with similar boundary conditions and geometry, the ultimate strength of the weld would be subject to a considerable reduction for the design engineer. Table 14 shows the statistical analysis summary for the weldment bending experiment, clearly indicating a difference in strength reduction between the two thicknesses.

Table 14. Allowable stress factor summary statistics for fillet weld bending experiment.

Two-Sample T-Test

Sample	Mean	Std Dev	P-Value	t-Value	DF	Min	Max
A	0.10	0.01	p<0.001	-7.97	25	0.08	0.13
B	0.15	0.02	P<0.001	-7.97	25	0.11	0.19

4.6 Discussion

Considering all the test specimens from both samples, no significant outliers in loading strength performance were discovered from any imperfections or impurities within the welds. However, none of the thirteen test specimens that failed the post-break test inspection were outliers in the load data. Since the measurements were consistent between the passing test specimens and the failed test specimens, the same conclusions would have likely been drawn from the statistical tests using either the cleaned data or the raw data. Alternatively, welds that lacked large amounts of root fusion or had large slag inclusions and porosity would have likely demonstrated underperforming results, when compared to results achieved by specimens with sufficient welds.

Failure loads measured for each sample set yielded drastically different values, with consistent results measured from each specimen. The tee-joint test specimens constructed with thicker 0.375 in (9.3 mm) A36 steel material showed an average failure load of twice the average failure load of the

test specimens constructed with 0.250 in (6.3 mm) material. The difficulty was in telling how much of the difference in effective weld area between the two samples and the difference in base metal thickness influenced the ultimate load capacity. Due to the loading configuration, there could have been additional structural stability derived from the thicker materials, allowing the welded connection to withstand greater loads. The larger weld size, if properly constructed, did increase the amount of fusion into the base metals and would certainly have increased the strength of the connection. However, it is difficult to quantify the influence of these parameters between the two different plate thickness samples, requiring different weld sizes to comply with AWS D1.1 weld size specifications.

Two sizes of weld bending test specimens were fabricated to evaluate strength in bending. The number of test piece rejections based upon preliminary inspections was 13. While this was a fairly large number, it did not adversely affect the statistical analysis in this study, but it did demonstrate the difficulty associated with producing uniform test pieces for welding experimentation, and it confirmed the wisdom of the original researchers in having multiple welders produce test pieces for examination. Since 27 out of 39 test specimens passed inspection after destructive testing, it proved that visually appealing welds do not guarantee structural integrity. This experiment showed that welds with uniform and aesthetic appearance may not possess all the critical requirements for a structurally-sound weld. In general, the thicker test pieces did produce higher loadings than the thinner pieces, and they did so by an amount larger than the simple addition of more material might suggest. In this experiment, ultimate tensile strength reductions of 90% for sample A and 85% for sample B were determined by using the ultimate load capacity measured in the experiment and the measured effective weld area of each test specimen. It can be concluded that welds loaded in cantilevered bending configuration experience more stresses and are subject to failure at loading prematurely compared to that of shear load configurations, and certainly compared with transversely loaded fillet welds, which use the total rating of weld filler metal tensile strength for evaluating load capacity of a weld. It is clear why this type of load configuration is not recommended for use in design. When forced into use in a repair situation, the welder must use extreme care to produce good welds and include far longer weld runs than would normally be needed to handle similar loads in other configurations.

Additionally, the strength of a fillet welded connection increases significantly when it is welded on both sides of the joint. The tests in this experiment were all conFig.d with a single fillet weld on one side of the connection to follow the AWS test. A tee-joint welded properly on both sides of the joint will likely never fail in this testing configuration. The double-sided tee-joint test piece shown in Fig. 25 was also crushed in the MTS 150 t (136 mt) hydraulic press to illustrate the increased strength that the double fillet weld provides. When applying the maximum load to the double fillet welded test piece, there was permanent deformation, but no fracture at the weld. The amount of weld mass at the joint provided significant structural support to the base materials.

Fig. 25. Double fillet welded tee-joint as an indicator piece for the fillet weld bending experiment.

5. Conclusions

The findings from this work can be summarized that aesthetic welds are not always good welds; good design, best procedural practices, and quality assurance are necessary to manufacture a quality welded product. Appropriate material selection is important for proper load carrying capacity; thicker materials and deeper welds provide more load carrying area, respectively. Further testing of the welded joint cantilever bending scenario seems justified; in the meantime, the results from this study would seem to indicate that extreme caution should be used in any repair contemplating a single-sided weld, and a double-sided weld should be used in design and, where possible, within repairs.

Acknowledgements

The authors would like to acknowledge and thank Mr. Jeffrey Lynch of Purdue University Research Machine Services and Mr. Scott Brand of Purdue University Agricultural & Biological Engineering. Their assistance with this project has been essential to its completion. Additionally, Mr. Robert Hershberger of the Purdue University Civil Engineering Pankow Laboratory is thanked for his guidance in the testing of the sample pieces. Mr. Robert M. Stwalley IV is graciously thanked for his technical illustration support. Dr. Carol S. Stwalley is acknowledged for her statistical and editorial assistance on the paper. This research did not receive any specific grant funding from any agencies in the public, commercial, or not-for-profit sectors. However, the assistance of the Purdue University Agricultural & Biological Engineering department is gratefully acknowledged for its support over the years with graduate teaching assistance positions and faculty salaries. The mention of trade names or commercial products in this article is solely for the purpose of providing specific technical information and does not imply recommendation or endorsement by Purdue University. The findings and conclusions in this publication are those of the authors, and they should not be construed to represent any official Purdue University determination or policy. Purdue University is an equal opportunity / equal access organization.

References

[1] R. Budynas and K. Nisbett, Shigley's Mechanical Engineering Design, 11th ed., New York, NY: McGraw Hill, 2020.

[2] T. H. Brown, Jr., Marks' Calculations for Machine Design, New York, NY: McGraw-Hill, 2005.

[3] A. D. Deutschman, W. J. Michels and C. E. Wilson, Machine Design - Theory and Practice, New York, NY: Macmillan, 1975.

[4] G. W. Krutz, J. K. Schueller and P. W. Claar II, "Machine Design for Mobile and Industrial Applications," Warrendale, PA, Society of Automotive Engineers, Inc, 1994.

[5] T. J. McPheron and R. M. Stwalley III, "Engineering Challenges Associated with Welding Filed Repairs," in *Welding Principles and Application*, London, Great Britian, IntechOpen Limited, 2022.

[6] T. J. McPheron and R. M. Stwalley III, "Fillet weld strength analysis for canilever loading," in *ASABE 2023 AIM - Omaha Conference*, St. Joesph, Michigan, 2023.

[7] I. Gomez, A. Kanvinde, Y. K. Kwan and G. Grondin, "Strength and ductility of welded joints subjected to out-of-plane bending," 2008. [Online]. Available: https://www.aisc.org/globalassets/aisc/research-library/strength-and-ductility-of-welded-joints-subjected-to-out-of-plane-bending.pdf. [Last Accessed 25 May 2024].

[8] J. L. Dawe and G. L. Kulak, "Welded connections under combined shear and moment," *Journal of the Structural Division*, vol. 100, no. 4, pp. 727-741, 1974.

[9] D. K. Dwivedi, Fundamentals of Metal Joining, Singapore: Springer, 2022.

[10] H. B. Cary, Modern Welding Technology, New York, NY: Prentice Hall, 2002.

[11] Lincoln Electric Company, The Procedure Handbook of Arc Welding, Cleveland, OH: The Lincoln Electric Company, 2000.

[12] S.-H. Kim, C.-H. Lee, I. Ryu and S. Park, "Experiemental investigation of cold formed high strength steel tubular joints subjected to moment loading," *Advances in Structural Engineering*, vol. 26, no. 12, pp. 2172-2198, 2023.

[13] A. H. N. Ateyah, "Bending stresses calculation in welded joint," *International Journal of Engineering Research and Applications*, vol. 12, no. 1, pp. 1-6, 2022.

[14] A. Santacruz and O. Millelsen, "Numerical stress analysis of tubular joints," in *Third Conference of Computational Methods & Ocean Technology - Stavanger*, Bristol, UK, 2021.

[15] T. Bjork, A. Ahola and T. Skriko, "On the distortion and warping of cantilever beams with hollow section," *Welding in the World*, vol. 64, pp. 1269-1278, 2020.

[16] F. I. Islamovic, P. Muratovic, D. Gaco and F. Kulenovic, "Bend testing of the welded joints," in *7th International Scientific Conference on Production Engineering (RIM 2009) - Cairo*, Bihac, Bosnia & Herzegovina, 2009.

[17] W. Qiu-dong, W. Yang, F. Zhong-qiu and W. Yi-xun, "Parametric study on fatigue failure modes of the rib-deck weld under out-of-plane bending loading," *Iranian Journal of Science and Technology, Transactions of Civil Engineering*, vol. 47, pp. 2625-2637, 2023.

[18] Y. Banno and K. Kinoshita, "Experimental investigation of fatigue strength of out-of-plane gusset welded joints under variable amplitude plate bending loading in long life region," *Welding in the World*, vol. 66, pp. 1883-1896, 2022.

[19] G. Prayogo, M. A. Budiyanto and M. Perkasa, "Analysis of bending mechanical performance of welding joints with the addition of diamond and circular plates," *Indonesian Journal of Engineering and Science*, vol. 4, no. 1, pp. 57-73, 2023.

[20] N. A. Husaini, J. K. Hamza and S. E. Sofyan, "Effects of welding on the change of microstructure and mechanical properties of low carbon steel," *Material Science and Engineering*, vol. 523, p. 012065, 2019.

[21] K. Hectors and W. De Waele, "Influence of weld geometry on stress concentration factor distribution in tubular joints," *Journal of Construction Steel Research*, vol. 176, p. 106376, 2021.

[22] E. Chouha, S. E. Jalal, Z. El Maskaoui and A. Chouaf, "Concentrated stress location areas for welded tubular T-joint under deflectedbending load," *MATEC Web of Conferences*, vol. 286, p. 02004, 2019.

[23] C. M. Mayr and K. Rother, "Improved stress concentration factors for circular shafts for uniaxial and combined loading," *Materials Testing*, vol. 61, no. 3, pp. 193-203, 2019.

[24] W. D. Pilkey and D. F. Pilkey, Peterson's Stress Concentration Factors, John Wiley & Sons, Inc., 2008.

[25] L. W. Zachary and C. P. Burger, "Stress concentrations in double welded partial joint penetration butt welds,"

Welsing Research Supplement, vol. 55, no. 3, pp. 77-82, 1976.

[26] K. Hectors and W. De Waele, "Cumulative damage and life prediction models for high-cycle fatigue of metals: a review," *Metals,* vol. 204, no. 11, 2021.

[27] A. Hobbacher, International Institute of Welding: Recommendations for Fatigue Design of Welded Joints and Components, Cham, Switzerland: Springer International Publishing, 2016.

[28] A. Hobbacher and M. Kassner, "On relation between fatigue properties of welded joints, quality criteria and groups in ISO 5817," *Welding in the World,* vol. 56, pp. 153-169, 2012.

[29] B. Jonsson, J. Samuelsson and G. B. Marquis, "Development of weld quality criteria based on fatigue performance," *Welding in the World,* vol. 55, pp. 79-88, 2011.

[30] S. I. Talabi, O. B. Owolabi, J. A. Adebisi and T. Yahaya, "Effect of welding variables on mechanical properties of low carbon steel welded joint," *Advances in Production Engineering & Management,* vol. 9, no. 4, pp. 181-186, 2014.

[31] S. P. Tewari, A. Gupta and J. Prakash, "Effect of welding parameters on the weldability of material," *International Journal of Engineering Science and Technology,* vol. 2, no. 4, pp. 512-516, 2010.

[32] T. R. Mupoperi and M. Pita, "An investigation of the effect of welding current on the mechanical properties of mild steel joints when using arc welding," in *IEEE 13th International Conference on Mechanical and Intelligent Manufacturing Technologies - Cape Town*, Piscataway, NJ, 2022.

[33] D. Pathak, R. P. Singh, S. Gaur and V. Balu, "Experimental investigation of effects of welding current and electrode angle on tensile strength of shielded metal arc welded low carbon steel plates," *Materials Today: Proceedings,* vol. 26, pp. 929-931, 2020.

[34] S. Y. Merchant, "Investigation on effect of welding current on welding speed and hardness of haz and weld metal of mild steel," *International Journal of Research in Engineering and Technology,* vol. 4, no. 3, pp. 44-48, 2015.

[35] R. Schiller, M. Oswald, J. Neuhausler, K. Rother and I. Engelhardt, "Fatigue strength of partial penetration butt welds of mild steel," *Welding in the World,* vol. 66, pp. 2563-2584, 2022.

[36] Y. Tobe and F. V. Lawrence, Jr., "Effect of inadequate joint penetration on fatigue resistance of high-strength structural steel welds," *Supplement to the Welding Journal,* vol. 9, pp. 259-266, 1977.

[37] T. R. Higgins and F. R. Preece, Proposed Working Stresses for Fillet Welds in Building Construction, vol. 6, Engineering Journal, American Institute of Steel Construction, 1969, pp. 16-20.

[38] American Bureau of Welding, "Report of the Structural Steel Welding Committee," American Welding Society, Miami, Florida, 1931.

[39] American Welding Society, AWS D1.1 Structural Welding Code - Steel, Miami: American Welding Society, 2020.

[40] American Welding Society, "AWS B4.0:2016 Standard Methods for Mechanical Testing of Welds," American Welding Society, Miami, 2016.

[41] Miller Electric Manufacturing, LLC, "Multimatic® 255 Multiprocess Welder w/ EZ-Latch™ Dual Cylinder Running Gear & TIG Kit - 208-575V," [Online]. Available: https://www.millerwelds.com/equipment/welders/mig-gmaw/multimatic-255-multiprocess-welder-m30175. [Last Accessed 15 May 2024].

[42] O. W. Blodgett, Design of Welded Structures, The James F. Lincoln Arc Welding Foundation, 1972.

[43] Canadian Welding Bureau, "Electrode Certifications," 2023. [Online]. Available: https://www.cwbgroup.org/safety/industry/electrode-certification. [Last Accessed 1 May 2023].

[44] Z. Barsoum and M. Khurshid, "Ultimate Strength Capacity of Welded Joints in High Strength Steels," *Procedia Structural Integrity,* vol. 5, pp. 1401-1408, 2017.